Components and targets of the PINOID signaling complex in Arabidopsis thaliana

Zago, Marcelo Kemel

Chapter 3

A BTB/POZ domain protein-kinesin complex is likely to provide polarity to PINOID kinase signaling

Marcelo Kemel Zago, Douwe Doevendans, Remko Offringa

SUMMARY

The Arabidopsis PINOID (PID) protein serine/threonine kinase regulates plant development by modulating the polar transport of the phytohormone auxin (polar auxin transport or PAT). We have demonstrated that PID directs PAT by regulating the baso-apical subcellular localization of the PIN auxin efflux facilitators. To further investigate the PID signaling pathway we performed a series of yeast two-hybrid screens and found that PID interacts with the BTB/POZ domain protein PINOID BINDING PROTEIN 2 (PBP2), and that PBP2 interacts with several proteins, amongst which two paralogous plant-specific microtubule motor proteins. Here we describe a more detailed study of the interaction of PBP2 with the motor proteins PBP2 BINDING KINESIN 1 (PBK1) and 2 (PBK2). *In vitro* pull down and phosphorylation assays suggested that PBP2 functions as a scaffold protein, since the PBKs bind the C-terminal TAZ domain portion and the PID kinase binds the N-terminal BTB/POZ domain portion of PBP2. The possible existence of such a protein complex at the cytoplasm-plasma membrane boundary was corroborated by the overlapping spatio-temporal expression of *PID, PBP2* and the *PBKs*, and by the fact that the proteins - when fused to GFP – co-localize in the cytoplasm of Arabidopsis protoplasts. Analysis of *pbk1/pbk2* mutant plants and *35S::PBK1* overexpression lines showed phenotypes that were also observed in mutants defective in PAT and in *pid* loss-of-function seedlings, respectively. These observations suggest that the PBKs are involved in the suppression of PID or PID-like kinase activity. As PBP2 was shown to inhibit PID activity *in vitro*, we propose that PBK1 and PBK2 act as the transporters of PBP2 that result in asymmetric subcellular suppression of PID and PID-like activity at the cytoplasm-plasma membrane boundary, thereby providing polarity to the signaling of these kinases.

Abbreviations: ARF-GEF, ADP-ribosylation factor-GTP exchange factor; BTB/POZ, bric-a-brac, tramtrack and broad complex/Pox virus and zinc finger domain; CC, coiled-coil domain; C-kinesin, C-terminal motor kinesin; F-actin, actin filament; GFP, green-fluorescent protein; GST, glutathione-S-transferase; IAA, indole-3-acetic acid; MBP, myelin basic protein; M-kinesin, middle motor kinesin; MT, microtubules; N-kinesin, N-terminal motor kinesin; PAT, polar auxin transport; PBK, PBP2 binding kinesin; PBP, pinoid binding protein; PID, pinoid; PM, plasma membrane; TAZ, transcriptional adaptor putative zinc finger domain

INTRODUCTION

The plant cellular cytoskeleton is a versatile structure. It is required for a variety of functions, such as organelle positioning, cytokinesis, intra- and intercellular trafficking and signaling. The two main components of the plant cytoskeleton are actin filaments (F-actin) and microtubules (MT) (1). A great variety of proteins

associate with the cytoskeleton, but it is believed that molecular motors such as myosins and kinesins are most essential for F-actin and MT function, respectively.
Myosins share a head domain with ATPase activity that binds to F-actin and moves along the filament upon ATP hydrolysis. Plant myosins have not been well studied, but it is generally assumed that these motor proteins have similar functions as their orthologs in other organisms, such as reorientation of MT through F-actin, the control of intercellular transfer of macromolecules through plasmodesmata, transport of secretory vesicles to the plasma membrane, phragmoplast organization and deposition of cell wall material (2-7).
Kinesins also share a motor domain with ATPase activity, but differently than myosins, these proteins bind to and move over MT. Plant kinesins have been studied in more detail and the function of some of them is quite well understood. It has been shown, for example, that plant kinesins with the motor domain positioned at their carboxy-terminus (C-kinesins) move from the plus to the minus end of MT. C-kinesins participate in MT organization at spindle poles and midzone during meiosis and mitosis (Arabidopsis KATA and ATK5) (8, 9), in MT stabilization of cortical arrays in interphase cells (Arabidopsis and cotton KCBP) (10), and act as putative MT and F-actin cross-linkers (cotton KHC) (11). Interestingly, the protein KIN13A is the only partly characterized Arabidopsis internal motor domain containing kinesin (M-kinesin), and its motility has been characterized as plus end directed. KIN13A was demonstrated to associate with Golgi stacks, but it did not have MT de-polymerizing activity, as shown for M-kinesins of animal cells (12). Most of the characterized plant kinesins belong to the group of the N-kinesins, which have an amino-terminal motor domain and move from the minus to the plus end of MT. N-kinesins were shown to be involved in the orientation of cellulose microfibril deposition (Arabidopsis FRA1) (13), organization of MT at the phragmoplast (Arabidopsis PAKRP1 and PAKRP1L) (14), delivery of Golgi vesicles to the phragmoplast (Arabidopsis PAKRP2) (15), and cell plate formation during mitotic (Arabidopsis NACK1) (16, 17) and meiotic cytokinesis (Arabidopsis NACK2) (18). One of the best characterized N-kinesins is the tobacco NACK1. NACK1 was found to interact with and thereby activate the MAPKK kinase NPK1 at the phragmoplast during cell division (16).
From the few specific examples described above, and many other observations in different organisms, it can be deduced that one particular F-actin- and MT-dependent mechanism must be governed by the action of molecular motors: the intracellular trafficking of macromolecules and vesicles (19, 20). Interestingly, polar transport of the plant hormone auxin (polar auxin transport, or PAT) has also been shown to be dependent on cytoskeleton-mediated intracellular trafficking. PAT is facilitated by a family of transporter-like PIN proteins that show a polar subcellular localization that correlates with the direction of transport (21, 22). Geldner and co-

workers showed that in interphase cells PIN1 loaded vesicles travel to and from the plasma membrane (PM), and that this cyclic trafficking depends on F-actins (23). Recently it was found that the Arabidopsis myosin XI is possibly involved in this process (24). MTs have also been shown to be essential for PIN targeting. For example, Boutté and co-workers (25) showed that MT, and probably its associated proteins, are indirectly required for the polar localization of PINs. During cytokinesis, PIN1 accumulation at the cell plate also seems to be MT-dependent (23).

Our knowledge on the signaling mechanisms governing PIN targeting and cyclic trafficking of PIN vesicles is still limited. On one hand, proper polar deposition of PIN1 at the PM was found to depend on the BFA sensitive ADP Ribosylation Factor GDP/GTP Exchange Factor (ARF-GEF) GNOM (26, 27). On the other hand, we have demonstrated that PIN1 polar targeting is directed to the apical (top) side of the cell by the activity of the protein serine/threonine kinase PINOID (PID) (28).

To further elucidate the mechanism underlying PIN polar targeting, we performed a yeast two-hybrid screen for proteins interacting with PID. Interestingly, one of the PID binding proteins, the PINOID Binding Protein 2 (PBP2), was found to localize at the cortical cytoskeleton in onion cells (29). PBP2 has two protein-protein interaction domains, an amino-terminal Bric-a-brac, Tramtrack and Broad Complex/Pox virus and Zinc finger (BTB/POZ) domain, and a carboxy-terminal Transcriptional Adaptor putative Zinc Finger (TAZ) domain. This feature suggests that PBP2 possibly acts as scaffold protein that organizes protein complexes. *In vitro* pull down assays indicated that PID binds to the BTB/POZ domain containing part, and a yeast two hybrid screen for PBP2 interacting proteins revealed several proteins that interact with the TAZ domain-containing part (see Chapter 2).

Here we describe the functional analysis of two of these proteins, which are the paralogous N-kinesins PBP2 Binding Kinesin 1 and 2 (PBK1 and PBK2), in the context of their putative role in PID signaling. Our data suggest that PID, PBP2 and the PBKs are expressed in the same tissues in Arabidopsis and that they co-localize in the cytoplasm. Moreover, *in vitro* phosphorylation assays indicated that PID does not phosphorylate the PBKs or PBP2, suggesting that these proteins may be involved in regulating PID activity. The analysis of *pbk1/pbk2* loss-of-function mutants revealed that these plants are slightly defective in root growth and gravitropic response. Interestingly, PBK1 gain-of-function seedlings display an enhanced frequency of cotyledon abnormalities, a phenotype also observed in *pid* loss-of-function seedlings. Our observations indicate that the *in vivo* formation of a PID-PBP2-PBK protein complex is plausible and that PBKs are possibly involved in repressing PID or PID-like activity.

MATERIALS AND METHODS

Molecular cloning and constructs

Molecular cloning was performed following standard procedures (30). The yeast two-hybrid bait plasmid pAS2-PBP2 was obtained by cloning a *PBP2 PstI/SalI*-blunted fragment derived from pSDM6014 into pAS2 digested with *PstI/XmaI*-blunted. The histidine tagged PID construct was created by excising the *PID* cDNA with *XmnI-SalI* from pSDM6005 (29) and cloning it into pET16H (pET16B derivative, J. Memelink, unpublished results) digested with *BamHI*, blunted and subsequently digested with *XhoI*. The *35S::PID-GFP* construct was generated by amplifying the *PID* cDNA using the primers 5'-TTAATATGACTCACTATAGG-3' and 5'-GCTCACCATAAAGTAATCGAACGC-3' and the *eGFP* coding region using the primers 5'-GATTACTTTATGGTGAGCAAGGGC-3' and 5'-TCAATCTGAGTACTT GTACAG-3'. Both PCR products were used together with outer primers in a new PCR reaction to generate the *PID-GFP* fragment, which was cloned into pUC28 digested with *NcoI/HincII*. The resulting pUC28-PID-GFP was digested with *EcoRI/StuI*-blunted and the *PID-GFP* fragment was ligated into *EcoRI/SmaI* digested pART7. Construction of histidine- and GFP-tagged PBP2 vectors are described by Benjamins (29). The GST-tagged PBP2 fusion (plasmid pGEX-*PBP2*) was generated by digesting pSDM6014 (29) with *XhoI/SmaI* and cloning the *PBP2* cDNA into pGEX-KG (31). The plasmid for production of a GST-tagged PBP2 BTB/POZ domain was created by digesting pGEX-*PBP2* with *NdeI,* filling in with Klenow and re-ligating. This created a stop codon at position 220 aa of the protein. The plasmid encoding the GST-tagged PBP2 TAZ domain was created by deleting the *NcoI* fragment encoding the BTB/POZ domain from pGEX-*PBP2*. The *PBK1* and *PBK2* cDNAs were amplified using respectively the primer pairs PBK1F (5'-ACGCAAGTCGACAATATGGAGAAGACACAGATGCC-3') and PBK1R (5'-CGGGATCCAATCAGAGGAAATGAAATGACACC-3'), and PBK2F (5'-GGGAATTCCATATG ATGGGAGCGATTGCTGGAGAAG-3') and PBK2R (5'-GTCCTTTCCATATGCCATTATATGAACGTG GTTG-3'). The amplified *PBK1* cDNA was digested with *SalI/BamHI* and cloned into the corresponding restriction sites in pUC28. The *PBK2* cDNA PCR product was digested with *NdeI* and cloned into the corresponding restriction site in pUC28. The *GFP-PBK1* fusion was constructed by excising *PBK1* from pUC28 with *SalI/NotI* and cloning this fragment into the *XhoI/NotI* sites of $pTH2^{BN}$ (derived from the pTH2 plasmid described by Chiu and co-workers) (32). Histidine tagged PBK1CT and PBK2CT expression vectors were created by excising *PBK1CT* and *PBK2CT* from the pACT2-PBK1CT and pACT2-PBK2CT yeast two-hybrid clones with *NdeI/XhoI* and cloning these fragments into the corresponding restriction sites in pET16B (Novagen). *35S::PBK1* was constructed by cloning a *PBK1 SalI/BamHI* fragment into the *XhoI/BamHI* site of pART7. *35S::PBK1CT* and *35S::PBK2CT* were created by cloning *BglII* fragments comprising *PBK1CT* and *PBK2CT* from the pACT2 yeast two-hybrid clones into the *BamHI* site of pART7. All *35S::PBK* constructs were transferred as *NotI* fragments from pART7 into pART27 (33).

Yeast two hybrid screen

Using the Matchmaker II yeast two-hybrid system and *Saccharomyces cerevisiae* strain PJ69-4A (Clontech), an *Arabidopsis thaliana* cDNA library fused to the GAL4 activation domain (pACT2) was screened at 20°C with PBP2 fused to the GAL4 DNA binding domain (pAS2) as bait. The cDNA library was constructed from RNA samples isolated from Arabidopsis root cultures in a one to one mix of untreated roots and roots treated for 24 hours with the auxin analog 1-naphthaleneacetic acid (1-NAA) (34). The positive clones were analyzed by colony hybridization as described in the Hybond-N+ Membrane Manual (Amersham Biosciences) and in the work of Memelink and co-workers (35).

In vitro pull down experiments

GST tagged full-length PBP2, its deletion versions (GST-BTB/POZ and GST-TAZ) or GST protein alone were used in pull down assays with histidine (his)-tagged PBK2CT (H-PBK2CT). Cultures of *E. coli* strain BL21 containing one of the constructs were grown at 37ºC to OD_{600} 0,8 in 50 ml LC supplemented with antibiotics. The cultures were then induced for 4 hours with 1 mM IPTG at 30ºC, after which cells were

harvested by centrifugation (10 min. at 4.000 RPM in tabletop centrifuge) and frozen overnight at -20ºC. Precipitated cells were re-suspended in 2 ml Extraction Buffer (EB: 1x PBS, 2 mM EDTA, 2 mM DTT, supplemented with 0,1 mM of the protease inhibitors PMSF - Phenylmethanesulfonyl Fluoride, Leupeptin and Aprotinin, all obtained from Sigma) for the GST-tagged proteins or in 2 ml Binding Buffer (BB: 50 mM Tris-HCl pH 6,8, 100 mM NaCl, 10 mM $CaCl_2$, supplemented with PMSF 0,1 mM, Leupeptin 0,1 mM and Aprotinin 0,1 mM) for the his-tagged PBK2CT and sonicated for 2 min. on ice. From this point on, all steps were performed at 4ºC. Eppendorf tubes containing the sonicated cells were centrifugated at full speed (14.000 RPM) for 20 min, and the supernatants were transferred to fresh 2 ml tubes. H-PBK2CT supernatant was left on ice, while 100 µl pre-equilibrated Glutathione Sepharose resin (pre-equilibration performed with three washes of 10 resin volumes of 1x PBS followed by three washes of 10 resin volumes of 1x BB at 500 RCF for 5 min.) was added to the GST- fusion protein containing supernatants. Resin-containing mixtures were incubated with gentle agitation for 1 hour, subsequently centrifugated at 500 RCF for 3 min. and the precipitated resin was washed 3 times with 20 resin volumes of EB. Next, all H-PBK2CT supernatant (approximately 2 ml) was added to GST-fusions-containing resins, and the mixtures were incubated with gentle agitation for 1 hour. After incubation, supernatants containing GST resins were centrifugated at 500 RCF for 3 min., the new supernatants were discarded and the resins subsequently washed 3 times with 20 resin volumes of EB. Protein loading buffer was added to the resin samples, followed by denaturation by 5 min. incubation at 95^0C. Proteins were subsequently separated on a 12% polyacrylamide gel prior to transfer to an Immobilon^{TM}-P PVDF (Sigma) membrane. Western blots were hybridized using a horse radish peroxidase (HRP)-conjugated anti-pentahistidine antibody (Quiagen) and detection followed the protocol described for the Phototope-HRP Western Blot Detection Kit (New England Biolabs).

In vitro phosphorylation assays

All proteins used in *in vitro* phosphorylation assays were his-tagged for purification from several (usually five) aliquots of 50 ml cultures of *E. coli*. strain BL21 which were grown, induced, pelleted and frozen as described above for the *in vitro* pull down experiments. Each aliquot of frozen cells pellet was resuspended in 2 ml Lysis Buffer (25 mM Tris-HCl pH 8,0; 500 mM NaCl; 20 mM Imidazol; 0,1% Tween-20; supplemented with 0,1 mM of the protease inhibitors PMSF, Leupeptin and Aprotinin) and subsequently sonicated for 2 min. on ice. From this point on, all steps were performed at 4ºC. Sonicated cells were centrifugated at full speed (14.000 RPM) for 20 min, the new pellets were discarded, and supernatants from all aliquots of the same construct were transferred to a 15 ml tube containing 100 µl of pre-equilibrated Ni-NTA resin (pre-equilibration performed with three washes of 10 resin volumes of Lysis Buffer at 500 RCF for 5 min.). Supernatant and resin were incubated with gentle agitation for 1 hour. After incubation, supernatant containing Ni-NTA resin was centrifuged at 500 RCF for 3 min., the new supernatant was discarded and the resin subsequently washed: 3 times with 20 resin volumes of Lysis Buffer, once with 20 resin volumes of Wash Buffer 1 (25 mM Tris.Cl pH 8,0; 500 mM NaCl; 40 mM Imidazol; 0,05% Tween-20) and once with 20 resin volumes of Wash Buffer 2 (25 mM Tris-HCl pH 8,0; 600 mM NaCl; 80 mM Imidazol). In between the washes, the resin was centrifugated for 5 min. at 500 RCF. After the washing steps, 20 resin volumes of Elution Buffer (25 mM Tris.HCl pH 8,0; 500 mM NaCl; 500 mM Imidazol) was added to the resin and incubated for 15 min. with gentle agitation. The resin was centrifugated for 3 min. at 500 RCF, and the supernatant containing the desired protein was diluted a 1000-fold in Tris Buffer (25 mM Tris.HCl pH 7,5; 1 mM DTT) and concentrated to a workable volume (usually 50 µl) using Vivaspin micro-concentrators (10 kDa cut off, maximum capacity 600 µl, manufacturer: Vivascience). Glycerol was added as preservative to a final concentration of 10% and samples were stored at -80ºC.

Approximately 1 µg of each purified his-tag protein (PID and substrates) in maximal volumes of 10 µl were added to 20 µl kinase reaction mix, containing 1x kinase buffer (25 mM Tris-HCl pH 7,5; 1 mM DTT; 5 mM $MgCl_2$) and 1 x ATP solution (100 µM $MgCl_2$/ATP; 1 µCi ^{32}P-γ-ATP). Reactions were incubated at 30ºC for 30 min. and stopped by the addition of 5 µl of 5 x protein loading buffer (310 mM Tris-HCl pH 6.8; 10 % SDS; 50% Glycerol; 750 mM β-Mercaptoethanol; 0,125% Bromophenol Blue) and 5 min.

boiling. Reactions were subsequently separated over 12,5% acrylamide gels, which were washed 3 times for 30 min. with kinase gel wash buffer (5% TCA – Trichoroacetic Acid; 1% $Na_2H_2P_2O_7$), coomassie stained, de-stained, dried and exposed to X-ray films for 24 to 48 hours at -80ºC using intensifier screens.

Protoplast transformations

Protoplasts were obtained from *Arabidopsis thaliana* Col-0 cell suspension cultures that were propagated as described by Schirawski and co-workers (36). Protoplast isolation and PEG-mediated transformation followed the protocol described originally by Axelos and co-workers (37) and adapted by Schirawski and co-workers (36). The transformations were performed with 20 µg of plasmid DNA, after which the protoplasts were incubated for at least 16h. Images were obtained by laser scanning confocal microscopy.

Plant growth, -lines and -transformation

Seeds were germinated and seedlings grown on MA medium (38) supplemented with kanamycin 25 µg/ml or other compounds (for example, IAA 0,1 µM, NPA 0,3 µM) when required, at 21°C in 50% relative humidity and a 16 hours photoperiod of 2500 lux. Adult or flowering Arabidopsis plants were grown on substrate soil, in growth rooms at 20°C, 40% relative humidity and a 16 hours photoperiod of 2500 lux. The gravitropism assay was performed according to Luschnig and co-workers (39).
Arabidopsis mutant lines N506264 and N508956 with T-DNA insertions in *PBK1* and *PBK2*, respectively, were obtained from the Salk Institute. For the PCR identification of the mutant alleles we used primers 5'-TTCTCACCCTGACGTTCTGGC-3', 5'-GATTGCTGTCTTTGGCATGCTT-3' and 5'-TGGTTCACGTAG TGGGCCATCG-3' for *pbk1* allele N506264 and primers 5'-GCAAATCCTGAGCAAGCTCCAT-3', 5'-GCGATTGCTGGAGAAGAGCTG-3' and 5'- TGGTTCACGTAGTGGGCCATCG-3' for the *pbk2* allele N508956.
Binary vectors were transferred to *Agrobacterium tumefaciens* strain GV2260, and transgenic lines were obtained by the floral dip procedure (40).

Northern blot analysis

Total RNA extraction was performed using the RNeasy Plant Mini Kit (Quiagen). Northern blotting and hybridization were performed as described by Memelink and co-workers (35) with the following modifications: pre-hybridizations as well as hybridizations were conducted at 65°C using a new Pre-hybridization mix (10% Dextran Sulfate; 1% SDS; 1M NaCl; 50 µg/ml of Single Stranded Herring Sperm DNA). The final washing steps were performed at 42°C. *PBK1* and *PBK2* probes were synthesized using the *PBK1CT XmaI/SacI* and *PBK2CT NcoI/XhoI* cDNA fragments derived from the pACT2 yeast two-hybrid clones as templates. The probes were radio-labeled using the Prime-a-gene Labeling System Kit (Promega) and α-P^{32}-dCTP (Amersham).

RESULTS

PBP2 interacts with two paralogous kinesins

Two of the PBP2 interactors identified in the yeast two-hybrid screen described in Chapter 2 are paralogs belonging to the large family of sixty-one kinesins in Arabidopsis. The proteins were named PBK1 and PBK2 for PBP2 Binding Kinesin 1 and 2, respectively. The six cDNA clones that were picked up in the yeast two-hybrid screen, two for *PBK1* (At4g38950) and four for *PBK2* (At2g21300), all were partials encoding only the C-terminal portions PBK1CT and PBK2CT, respectively.

These results indicate that the C-terminal portion of the kinesins interacts with PBP2 (Figure 1A and 2).

To independently confirm the data from the yeast two-hybrid screen, *in vitro* protein pull down experiments were performed using affinity-purified histidine-tagged PBK2CT and GST-tagged PBP2 or GST-tagged versions of the BTB domain- or the TAZ domain containing portion of PBP2, respectively. These experiments showed that PBK2CT specifically interacts with the part of PBP2 that contains the TAZ domain (Figure 1B). Previously, we showed that PID interacts with the BTB domain containing portion of PBP2 (Figure 1, Chapter 2), and our current finding suggests that PBP2 may act as a scaffold protein, possibly forming a protein complex that comprises PBK1/2 and PID via its two interaction domains.

PBK1 and PBK2 belong to a plant specific clade of kinesins

Alignment of the PBK1 and 2 amino acid sequences showed that these proteins are very similar, sharing an overall amino acid identity of 81,6% (Figure 2). Protein domain analysis using ScanProsite software identified their motor domains to be located at the amino-terminus, suggesting a minus to plus-end motility on MT strands. Separate analysis of the different parts of the PBK proteins indicated that they share respectively 91% and 75,4% amino acid identity in their motor- and carboxy-terminal PBP2 interacting domains (Figure 1A and 2). A previous large scale comparison of kinesins from Arabidopsis and other organisms indicated that PBK1 and PBK2 belong to a plant specific clade that includes the proteins encoded by the genes At3g51150, At4g24170, At5g42490 and At5g66310, and the well-characterized kinesins AtNACK1 and 2 that were shown to be involved in cytokinesis (18, 41). Our own alignments using either the full length sequences or the motor domains of the Arabidopsis kinesins confirmed these results (Figure 1C). The eight clade members share four highly conserved domains: an amino-terminal motor domain, a single coiled-coil domain and two domains of unknown function in the carboxy-terminal region (Figure 1A). The hypothetical binding site for the Arabidopsis NPK1-ortholog (AtNPK1) (16) that is present in the carboxy-terminus of AtNACK1 and 2, could not be identified in other members of the clade (Figure 1A). This implies that AtNPK1 acts specifically on the AtNAKCs and not on the other kinesins of this clade.

The carboxy-terminal portions of PBK1 and 2 are not phosphorylated by PID

PBP2-dependent recruitment of PBK1 and PBK2 could function to alter their activity through phosphorylation by PID. To test this possibility, we performed *in vitro* phosphorylation assays using PID and PBK2CT or PBK1CT with or without PBP2 in separate reactions. The general phosphorylation substrate Myelin Basic Protein

(MBP) was used as a positive control. While strong phosphorylation of MBP could be detected, no significant PID-dependent phosphorylation of PBK1CT or PBK2CT was observed in these experiments, even in the presence of PBP2 (Figure 1D), indicating that CT domains of the kinesins are not targets for phosphorylation by PINOID. This observation, however, does not exclude the possibility that PID phosphorylates residues in the N-terminal part of PBK1/2. Interestingly, the presence of PBP2 reproducibly reduced the auto-phosphorylation activity of PID, which is in line with the proposed function of PBP2 as negative regulator of PID activity (Chapter 2).

The PBKs, PBP2 and PID are expressed in the same tissues and co-localize in the cytoplasm

Even though there is no data indicating that PBKs are phosphor-substrates of PID, they may still function in the PID signaling pathway. The kinesins could affect the subcellular localization or -activity of PID, or be involved in altering cytoskeletal properties as part of the PID-PBP2-PBK complex. Such functions require that the PBKs are co-expressed in the same cells and co-localize to the same subcellular compartments as PID and PBP2.

To assess the spatio-temporal expression of the corresponding genes, we compiled publicly available data from the Genevestigator and Arabidopsis MPSS databases (42, 43). Data extracted from the Genevestigator database indicated that both *PBKs* and *PID* reach highest expression levels at the bolting stage (Figure 3A, right), although these genes are also significantly expressed at rosette stage 1 (Figure 3A, right). In Arabidopsis tissues, high expression of the *PBKs* and *PID* coincides in flowers, more specifically in petals (Figure 3A, left). Interestingly, the expression pattern of *PBK2* is most similar to that of *PID*, with highest expression in the shoot apex (Figure 3A, left). In contrast to *PID*, the *PBKs* show a mild but significant expression in lateral roots and in the root elongation zone.

The expression data for the *PBKs* and *PID* in the Arabidopsis MPSS database partly corroborate those from Genevestigator, with highest mRNA abundance detected in the inflorescence (Figure 3B). Notably, *PBP2* expression appears to be minor in these organs, whereas it is very high in tissues where the other three mRNAs are not very abundant, such as leaves and roots (Figure 3B). Our and other studies have shown that *PBP2* expression reaches intermediate levels in inflorescences and floral organs (Robert *et al.*, unpublished data) (44, 45). These results indicate that *PID*, *PBK1*, *PBK2* and *PBP2* expression patterns overlap, in particular in the inflorescence where PID is known to play an important role.

To compare the sub-cellular localization of the PBKs with that of PID and PBP2, we transformed *35S::GFP, 35S::GFP-PBK1, 35S::PID-GFP* and *35S::GFP-PBP2* constructs to Arabidopsis protoplasts. Both GFP-PBK1 and PID-GFP predominantly

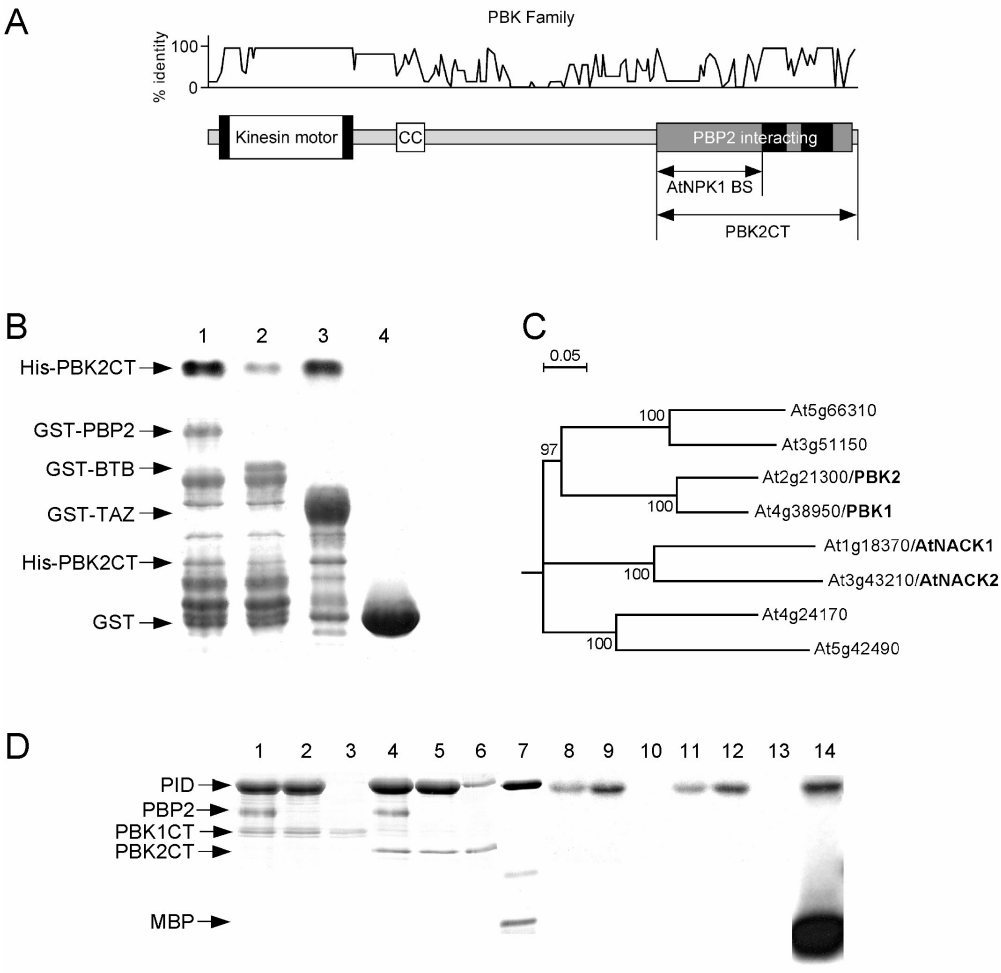

Figure 1. The plant specific kinesins PBK1 and PBK2 interact with PBP2 but are not phosphorylated by PID *in vitro*. (A) Graph showing the percentage of identity between the eight PBK clade members (upper part) in relation to their different conserved domains (lower part). Indicated are the kinesin motor domain, the coiled-coil domain (CC), the Arabidopsis NPK1-ortholog binding site (AtNPK1 BS) in AtNACK1/2, and the two PBK clade-specific PFam signatures (black boxes). Those PBK clade-specific domains are present in the region corresponding to the 258 amino acid PBP2-interacting C-terminal portion of PBK2 (PBK2CT) that was picked up in the yeast two-hybrid screen and subsequently used in the *in vitro* pull down. (B) Immuno-detection (top) and coomassie stained gel (bottom) of an *in vitro* protein pull down assay using his-tagged PBK2CT together with GST-tagged PBP2 (lane 1), GST-tagged BTB (lane 2) or TAZ domain containing portion (lane 3) of PBP2 or the GST protein alone (lane 4). (C) Phylogenetic tree showing the PBKs and their plant-specific relatives. Bootstrap values are indicated. (D) Coomassie stained gel (lanes 1 to 7) and autoradiograph (lanes 8 to 14) of an *in vitro* phosphorylation assay using PID (lanes 1, 2, 4, 5, 7, 8, 9, 11, 12 and 14), PBP2 (lanes 1, 4, 8 and 11), PBK1CT (lanes 1 to 3 and 8 to 10), PBK2CT (lanes 4 to 6 and 11 to 13) and MBP (lanes 7 and 14).

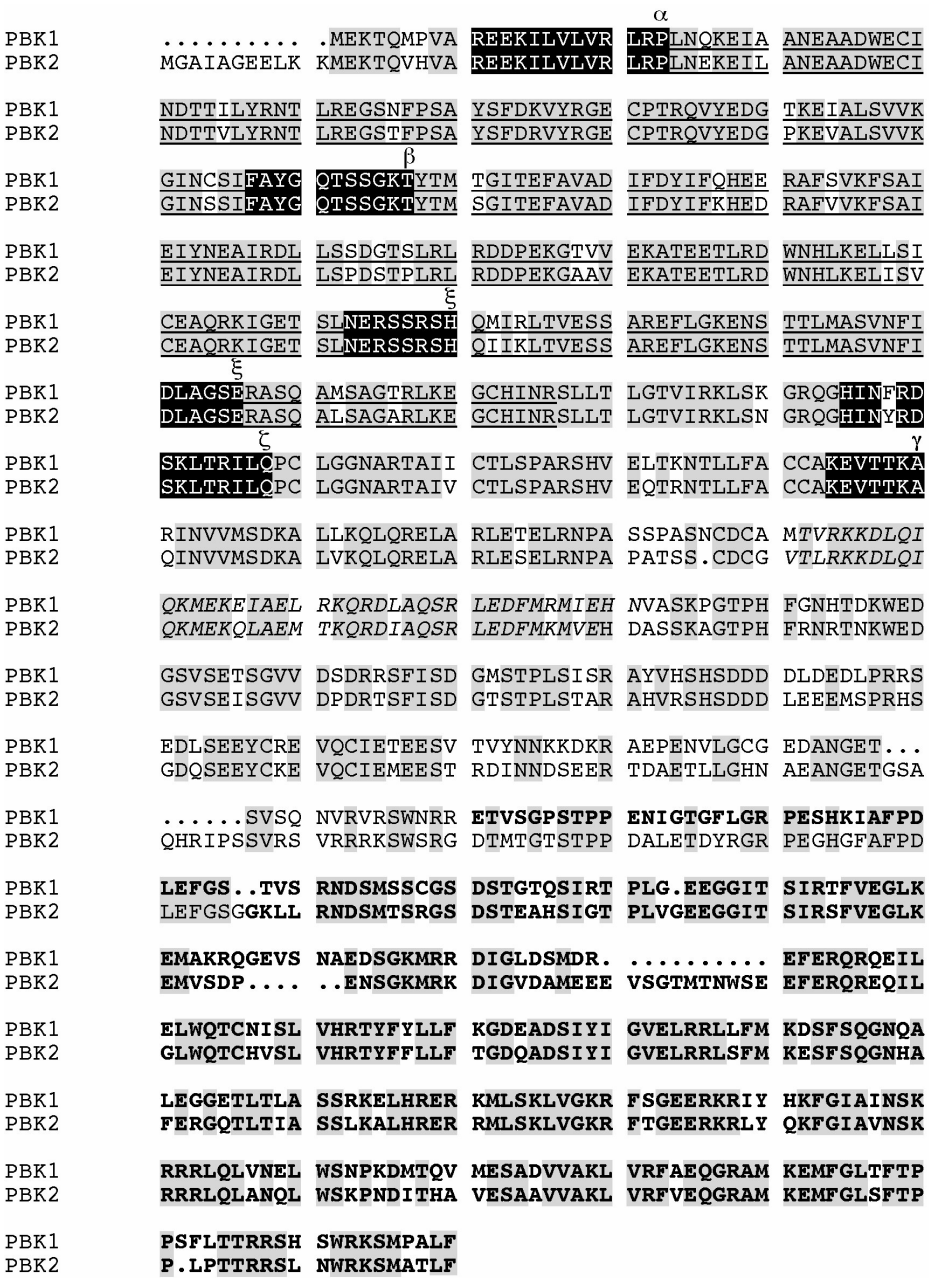

Figure 2. PBK1 and PBK2 are paralogous N-kinesins. PBK1 and PBK2 show 81,6% overall amino acid identity and 91% and 75,4% identity in the motor domain (underlined) and the carboxy-terminal PBP2-interacting region (bold), respectively. Identical amino acid residues are shown in gray shading. The coiled-coil domain is indicated in italics. Putative neck sequences (α, in which absence of the GN motif suggests MT plus-end motility, and γ), the ATP binding site (β) and other nucleotide phosphates binding sites (ξ) or the microtubule interacting site (ς) are shown in black shading.

localized to the PM, but some fluorescent signal was observed in the cytoplasm (Figure 3C). Notably, GFP-PBP2 localization varied between protoplasts: in 80% of the GFP positive protoplasts nuclear localization was observed, whereas 20% of those protoplasts showed a cytoplasmic fluorescent signal (Figure 3C and Chapter 2). Due to the even signal intensity through the cellular regions in the latter case, we can not exclude that part of GFP-PBP2 also localizes to the PM (Figure 3C).

In conclusion, the combined data allow us to speculate that the hypothesized PID-PBP2-PBK complex functions at the cytoplasm–PM boundary of cells in the inflorescence meristem to regulate organ development. The *in vivo* occurrence of such a complex remains however to be determined.

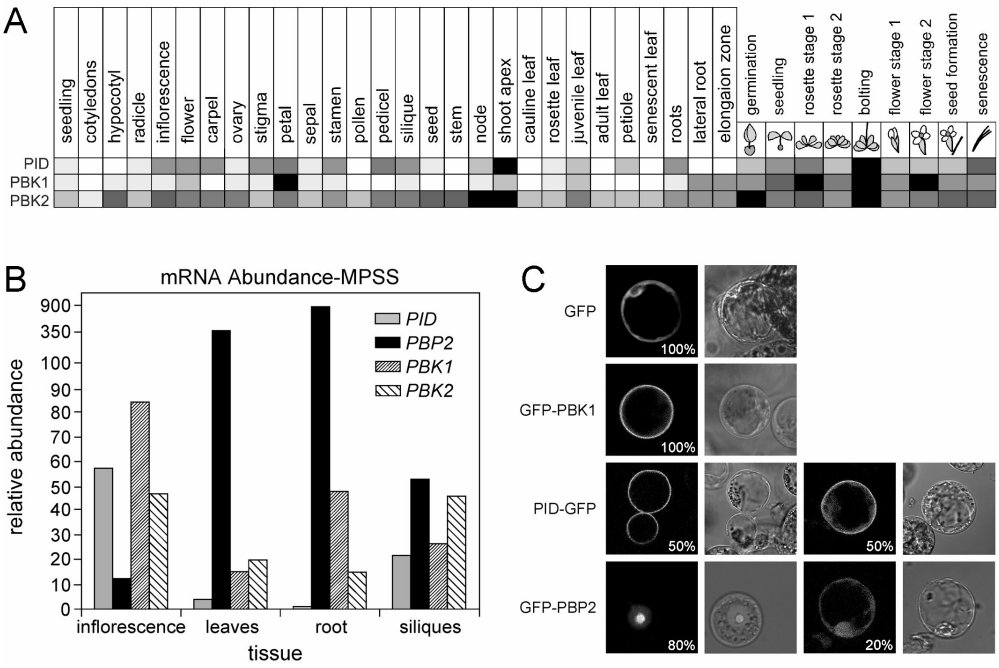

Figure 3. PBKs, PID and PBP2 are expressed in the same tissues and co-localize in the cytoplasm. (A) Expression profiles of *PID*, *PBK1* and *PBK2* in different Arabidopsis tissues (left) and developmental stages (right) according to Genevestigator Database. Black: tissue or developmental stage in which a certain gene reaches maximal expression; white: tissue or developmental stage in which a certain gene is not expressed; grayscale: intermediate expression levels. (B) Expression profiles of *PID*, *PBK1*, *PBK2* and *PBP2* in Arabidopsis tissues according to the Arabidopsis MPSS Database. (C) Confocal laser scanning and transmission light microscopy images (merged with fluorescent images) of representative Arabidopsis protoplasts transformed with *35S::GFP*, *35S::GFP-PBK1, 35S::PID-GFP* and *35S::GFP-PBP2*. The frequencies observed for the different localizations are indicated.

PBK1 and PBK2 act redundantly in the control of root growth

Assuming that one of the functions of PBK1 and 2 could be to regulate PID and that this action could be essential for proper PAT, it is possible that loss-of-function mutants for both kinesins show phenotypes related to defects in PAT, similar to plants with altered *PID* expression levels. Lines N506264 (*pbk1*) and N508956 (*pbk2*) were obtained from the Salk Institute and PCR analysis confirmed that the T-DNA insertions in these lines are in exons 9 and 4 of the *PBK1* and *PBK2* genes, respectively (Figure 4A). The complete knock-out of *PBK1* and *PBK2* transcription in such plants, however, could not be conclusively determined due to the very low expression levels of both genes in wild type seedlings (data not shown). Nevertheless, *pbk1* and *pbk2* were crossed in order to generate the *pbk1/pbk2* double mutant. Subsequently, the single and double *pbk* loss-of-function lines were subjected to detailed phenotypic analysis.

The single *pbk* mutants did not show significant phenotypic differences compared to wild type under standard growth conditions, both at the seedling and flowering stage. The *pbk1/pbk2* double mutant seedlings, however, showed a slight but statistically significant reduction in root elongation (Figure 4B) and a slower gravitropic root response compared to wild type (Figure 4C). At the flowering stage *pbk1/pbk2* plants were indistinguishable from wild type.

The observed reduced gravitropic response of *pbk1/pbk2* seedlings could indicate a possible role for both kinesins in the regulation of PAT in the roots. Interestingly, *PID* overexpression also results in agravitropic root growth, and although PID itself does not seem to have an apparent function in this organ, its overexpression may trigger the signaling pathway of some of its family members. In the view of the indirect link between the PBKs and PID, we interpret our results as an indication that the kinesins act redundantly in the control of root growth, possibly by repressing the activity of the PID kinase family members.

Overexpression of PBK1 leads to defects in cotyledon positioning

To further investigate the function of the PBKs, we tested overexpression of the full length *PBK1* cDNA and the 3' end of the *PBK* cDNAs encoding the PBP2 interacting C-terminal portions (PBK1CT and PBK2CT) under the control of the *CaMV 35S* promoter. With the latter constructs we expected to observe dominant negative effects, since it produces a non-functional protein that possibly titrates out PBP2 protein complexes.

Approximately twenty T2 lines carrying a single locus insertion of the constructs *35S::PBK1CT* and *35S::PBK2CT* were analyzed, but none of them showed obvious phenotypes, in spite of the fact that several of these lines showed strong overexpression levels (Figure 4D).

In seven of the nineteen *35S::PBK1* single locus lines, T2 seedlings with three or sometimes fused cotyledons were observed at frequencies ranging from 1:1000 in line *35S::PBK1-5* to 1:30 in line *35S::PBK1-3* (Table 1 and Figure 4E). Most of the *35S::PBK1* lines did not show any further defects at the rosette or flowering stage.

Table 1. PBK1 overexpression results in cotyledon defects

***Arabidopsis thaliana* line**	**Generation**	**Seedlings with abnormal cotyledons/total seedlings**	**Frequency of cotyledon abnormalities**
Columbia wild type	-	0/1740	< 0,05%
35S::PBK1-3	T2/T3	13/500	2,60 %
35S::PBK1-5	T2	1/1061	0,10 %
35S::PBK1-18-1	T2	2/557	0,35 %
35S::PBK1-19-2	T2	4/1346	0,30 %
35S::PBK1-19-3	T2	2/852	0,23 %
35S::PBK1-19-4	T2	2/656	0,30 %
35S::PBK1-21-2	T2	3/400	0,75 %
35S::PBK1-7	T3	0/500	< 0,20 %
35S::PBK1CT-13	T3	0/500	< 0,20 %
35S::PBK2CT-4	T3	0/500	< 0,20 %

For line *35S::PBK1-3*, however, one in four T2 plants developed short roots, had a dwarf stature and bolted with great delay, although not producing flowers (Figure 4F). The Mendelian segregation ratio and the fact that we were not able to generate homozygous T3 lines indicated that the plants with strong phenotypes were homozygous for the overexpression construct. Northern analysis showed that *35S::PBK1-3* seedlings contain very high *PBK1* expression levels compared to those of other *35S::PBK1* lines (Figure 4D). This strongly suggested that the frequent cotyledon phenotypes, and possibly also the dwarf phenotypes of homozygous *35S::PBK1-3* plants, are induced by high levels of *PBK1* overexpression. For these latter phenotypes we can not exclude, however, that they are the result of a loss-of-function mutation caused by the insertion of the overexpression construct. The cotyledon defects are however observed in multiple overexpression lines, and their frequency seems to correlate with the level of overexpression. Interestingly, *pid* mutant plants show similar cotyledon abnormalities, and the penetrance of the mutant phenotype has been correlated with the strength of the mutant *pid* allele (46). Our observations on the *PBK1* overexpression lines corroborate our previous hypothesis that the PBKs repress the activity of the PID protein kinase and its closely related family members. The low frequency of the *35S::PBK1* cotyledon defects could be due to the fact that the *CaMV 35S* promoter usually becomes active during embryonic stages where the cotyledons boundaries have already been defined. The use of promoters that are

active during early embryogenesis to drive ectopic *PBK1* expression should confirm our hypothesis.

DISCUSSION

The plant cellular cytoskeleton has been shown to play a crucial role in several important processes, including polar transport of the plant hormone auxin (PAT). PAT is mediated by the PIN auxin efflux facilitators, whose asymmetric distribution over the cell membrane correlates with the directionality of transport (47, 48). In interphase cells, the polar subcellular localization of PIN proteins requires indirect MT action and is maintained by cyclic trafficking of PIN loaded vesicles along the actin cytoskeleton, whereas localization of PIN1 to the cell plate during cytokinesis was found to be MT-dependent (23, 25, 27, 47, 48). Previously, we demonstrated that the protein serine/threonine kinase PINOID (PID) is a key regulator of the apico-basal polarity of PIN proteins (28). PID was found to interact with the BTB/POZ domain protein PBP2 that - when fused to GFP - showed a possible cytoskeletal localization in onion cells (29). The data presented in this chapter suggest that PBP2 interacts with two homologous Arabidopsis kinesins PBK1 and PBK2, and that the PBP2-PBK complex is involved in the regulation of PID activity. Our findings provide the first clues for a third MT-dependent pathway in the regulation of the subcellular localization of PIN proteins.

The plant-specific N-kinesins PBK1 and PBK2 may be part of the PID signaling complex

Alignment of PBK1 and 2 with the other fifty-nine kinesins encoded by the Arabidopsis genome showed that they cluster in a plant specific clade of eight kinesins that are characterized by the presence of two unique conserved carboxy-terminal domains. Except for AtNACK1 and 2, which have been characterized as essential for the completion of cytokinesis during mitosis and meiosis (16-18), not much is known about the function of the other clade members.

The yeast two-hybrid data and *in vitro* pull down experiments indicate that PBP2 interacts with the C-terminal region of PBK1 and PBK2. The fact that this region contains domains that are conserved among PBK-like proteins allows the possibility that PBP2 interacts with other kinesins of the PBK/NACK clade. This is likely to be the case, as the lack of strong mutant phenotypes in the *pbk1pbk2* double mutant indicates functional redundancy among the members of the PBK/NACK clade. On the other hand, the C-terminal AtNPK1 binding domain is only present in AtNACK1 and 2 and not in other members of the PBK/NACK clade, which illustrates that some PBK relatives also have their specific, unrelated function. Since it is believed that C-

terminal domains of kinesins are involved in cargo binding, it is logical to assume that PBP2 is the cargo of PBK1/2 and possibly also the cargo of PBK relatives.

Our findings that PID and the PBKs interact with different protein interaction domains of PBP2, and that PID and PBK1 predominantly localize at the PM but that the three proteins co-localize in the cytoplasm, led us to speculate that these proteins form a regulatory complex at the cytoplasm-PM boundary. The overlapping expression patterns of *PID, PBP2* and the *PBKs* seem to corroborate this hypothesis. However, the existence of a functional PID-PBP2-PBK protein complex requires further *in vivo* confirmation.

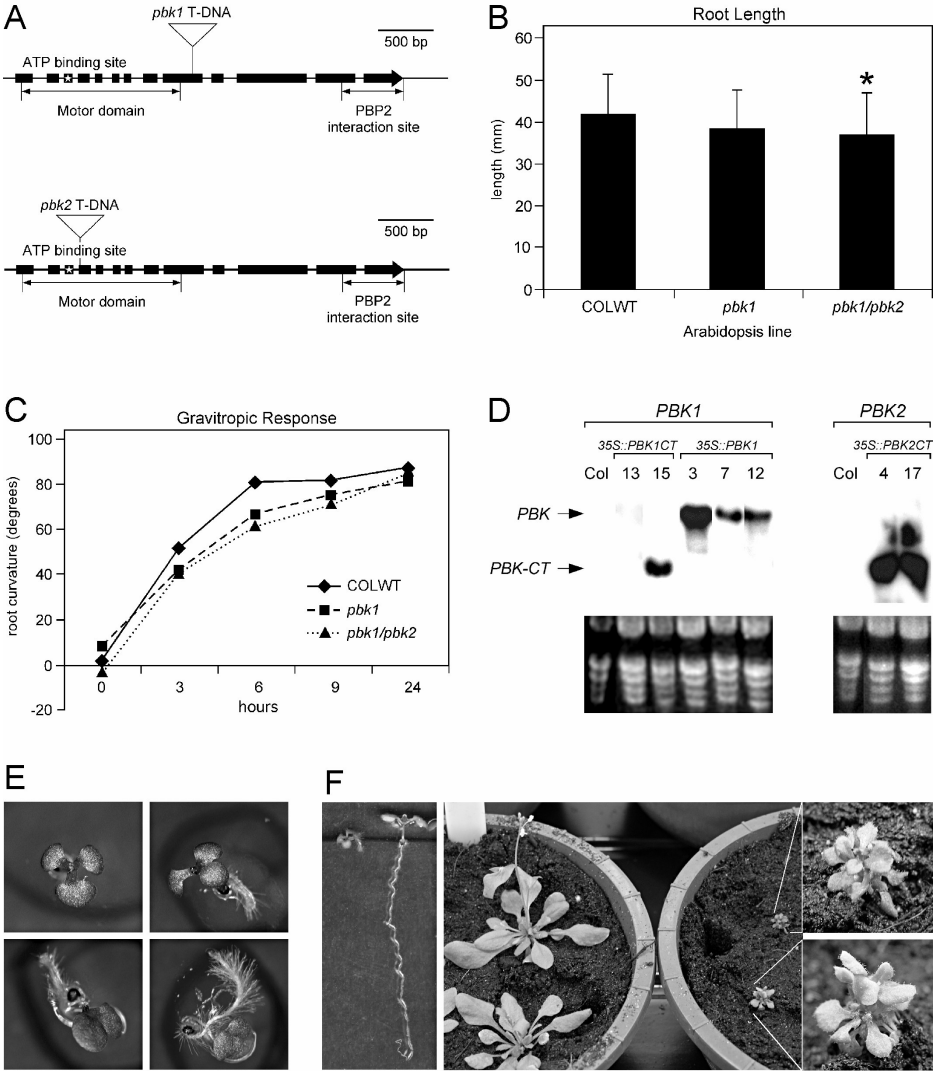

Figure 4. PBK1 and 2 act redundantly in the control of root growth and their overexpression affects cotyledon positioning. (A) Schematic diagram of the *PBK1* and *PBK2* genes indicating the T-DNA insertion sites in *pbk1* and *pbk2*. Boxes represent exons. The regions encoding the putative motor domain, the ATP binding site (star), and the PBP2 interaction site are indicated. (B) Ten-day-old seedlings of the *pbk1/pbk2* double mutant, but not of the *pbk1* single mutant, develop statistically significant shorter roots (star) compared to Columbia wild type (COLWT; Student's t-test t=2,5; p>0,05; n = 40 for COLWT and n=78 for *pbk1/pbk2*). (C) Gravitropic response of COLWT, *pbk1* and *pbk1/pbk2* seedlings. Seedlings were grown for 5 days on vertically oriented plates, after which the plates were rotated 90°. The curvature of the root tips with the horizontal axis was monitored in time. At 6 and 9 hours post-reorientation, the roots of *pbk1/pbk2* showed statistically significant reduced curvature compared to COLWT (Student's t-test: for 6h t=2,93, p>0,05, n=39 for COLWT and n=63 for *pbk1/pbk2*; for 9h: t=2,61, p>0,05, n=37 for COLWT and n=60 for *pbk1/pbk2*). (D) Top panel: autoradiograph of a Northern blot of total RNA from 7-day-old seedlings of Columbia wild-type (Col), and of different *35S::PBK1, 35S::PBK1-CT* and *35S::PBK2-CT* lines after hybridization with the *PBK1* and *PBK2* cDNA probes. Bottom panel: ethidium bromide stained gel. (E) *35S::PBK1* lines produce a significantly enhanced number of seedlings with cotyledon malformations. (F) Homozygous *35S::PBK1-3* seedlings (left picture; left seedling) show cotyledon defects combined with dwarf stature. These dwarf plants bolt with great delay but do not flower (middle picture; plants on the left are wild type looking heterozygous *35S::PBK1*-3 plants; bushy plants on the right and inset are homozygous *35S::PBK1*-3 plants).

PBK1 and PBK2 are possible regulators of PID activity

In this chapter we show that altered levels of PBK expression lead to discrete phenotypes that are also observed in Arabidopsis mutants that are defective in auxin transport. Roots of the *pbk1/pbk2* double mutant are slightly shorter and agravitropic compared to those of wild type plants. The mild phenotypic effects are probably due to the functional redundancy within the PBK clade. Triple and quadruple mutants in *PBK1*, *PBK2*, and their closest homologs are currently being generated to test this hypothesis. Furthermore, overexpression of *PBK1* under control of the *CaMV 35S* promoter resulted in defects in cotyledon positioning. Several independent *35S::PBK1* lines produced seedlings with three or fused cotyledons, a phenotype that is typically observed in *pid* loss-of-function mutants.

One of the *35S::PBK1* lines displayed severe phenotypes: seedlings had a dwarf stature and very short roots, and adult plants developed into bushy dwarfs that did not flower. The phenotypes of these plants resemble those of gibberellic acid (GA) or brassinosteroid biosynthesis or insensitive mutants (*ga1-3*, *det2, bri1, bin1* or *bin2*) (49-51). Interestingly, this particular line showed a very high level of *PBK1* overexpression, and segregation analysis suggested that the phenotypes were only observed in plants that are homozygous for the T-DNA insert. It is tempting to speculate that the observed phenotypes are dose dependent, and therefore only observed with above-threshold levels of *PBK1* overexpression. At this stage, however, we can not exclude that the phenotypes are the result of a recessive loss-of-function mutation caused by insertion of the overexpression T-DNA construct, possibly in a gene involved in brassinosteroid or GA signaling or biosynthesis.

In spite of the inconclusive phenotypes of the homozygous *355S::PBK1-3* plants, the tricotyledon phenotype is observed in several independent overexpression lines, with a highest frequency in the strong *355S::PBK1-3* line. In this respect, *PBK1* gain-of-function plants mimic *pid* loss-of-function mutants. The relatively low frequency of tricotyledon seedlings (2,6% in line *35S::PBK1-3* versus 10-50% in *pid* mutants alleles) may relate to the use of the *35S* promoter, which comes on relatively late during embyogenesis, mostly at stages where cotyledon primordia have already been established. In order to obtain more conclusive data on the effect of *PBK1* overexpression on embryo development, we are currently analyzing plants that express the *PBK1* cDNA under control of the *RPS5A* promoter that is highly active during early embryogenesis (52). As this promoter also provides high expression in meristems, we may find more lines that mimic the strong post-embryonic phenotypes of line *35S::PBK1-3*.

These results suggest that PBK1 and PID act antagonistically, but how is still unclear. From the *in vitro* phosphorylation experiments we can deduce that the PBP2-interacting C-terminus of PBK2 is not a phosphor-substrate of PID. Although new assays using the full length PBK proteins should determine whether other parts can be phosphorylated by PID, we hypothesize that PBKs – through their interaction with PBP2 – are rather involved in negatively regulating PID activity. Can we - based on this model - explain the mildly agravitropic and shorter roots observed for *pbk1/pbk2* double mutant seedlings? Both root growth and the gravitropic response of roots are depending on proper redistribution of auxin from the columella to the epidermal cells in the elongation zone of the root. This redistribution is mediated by the concerted action of PIN3 and PIN2, which redirect the auxin flow by their specific subcellular localization (53, 54). The observed phenotypic defects of the *pbk1/pbk2* seedlings could be the result of mis-localization of PIN2 and PIN3 due to a defect in repression of protein kinase activity by PBP2. As PID is not expressed in the root tip (55), it is most likely that PID-related protein kinases affect the PIN polarity in this organ. In line with this it was recently reported that loss-of-function mutants in *AtPK3/WAG1* and its closest homolog *AtPK3-like/WAG2* have a defective root waving response (56).

Concluding remarks

Although the results described in this chapter are far from being conclusive, they provide possible initial clues linking cytoskeletal-dependent intracellular trafficking to PID-mediated signaling in the control of PAT. We have identified two N-kinesins that could possibly play a role in this process by regulating the activity of PID and its family members. In the view of the possible interaction between PBP2 and the PBKs and the inhibitory effect of PBP2 on PID, it is plausible that the PBKs function

to transport PBP2 to repress the activity of PID or its related kinases in an asymmetric manner, thereby providing polarity to the signaling of these kinases.

ACKNOWLEDGEMENTS

This work was financially supported by CAPES (Brazilian Federal Agency for Post-Graduate Education, M. K.-Z.). We thank Bert van der Zaal for providing the root-specific cDNA library, Rene Benjamins for providing constructs pSDM6006 (H-PBP2), pSDM6014 (pBSSK-PBP2) and pSDM6025 (pTH2GFP-PBP2), Carlos Galvan for the plasmids encoding H-PID and PID-GFP, Johan Memelink for providing pET16H, Gerda Lamers for help with confocal laser scanning microscopy, Helene Robert for helpful comments on the manuscript, Peter Hock for art work, and the Salk Institute Genomic Analysis Laboratory for providing the sequence indexed Arabidopsis T-DNA insertion mutants *pbk1* and *pbk2*.

REFERENCE LIST

1. Kost, B., Bao, Y. Q. & Chua, N. H. (2002) *Philos. Trans. R. Soc. Lond B Biol. Sci.* **357**, 777-789.

2. Dong, C. H., Xia, G. X., Hong, Y., Ramachandran, S., Kost, B. & Chua, N. H. (2001) *Plant Cell* **13**, 1333-1346.

3. Schwab, B., Mathur, J., Saedler, R., Schwarz, H., Frey, B., Scheidegger, C. & Hulskamp, M. (2003) *Mol. Genet. Genomics* **269**, 350-360.

4. Hasezawa, S., Sano, T. & Nagata, T. (1998) *Protoplasma* **202**, 105-114.

5. Blackman, M. & Overall, L. (1998) *Plant Journal* **14**, 733-741.

6. Heinlein, M. (2002) *Curr. Opin. Plant Biol.* **5**, 543-552.

7. Jurgens, G. (2005) *Trends Cell Biol.* **15**, 277-283.

8. Chen, C., Marcus, A., Li, W., Hu, Y., Calzada, J. P., Grossniklaus, U., Cyr, R. J. & Ma, H. (2002) *Development* **129**, 2401-2409.

9. Ambrose, J. C., Li, W., Marcus, A., Ma, H. & Cyr, R. (2005) *Mol. Biol. Cell* **16**, 1584-1592.

10. Mathur, J. & Chua, N. H. (2000) *Plant Cell* **12**, 465-477.

11. Preuss, M. L., Kovar, D. R., Lee, Y. R., Staiger, C. J., Delmer, D. P. & Liu, B. (2004) *Plant Physiol* **136**, 3945-3955.

12. Lee, Y. R. & Liu, B. (2004) *Plant Physiol* **136**, 3877-3883.

13. Zhong, R., Burk, D. H., Morrison, W. H., III & Ye, Z. H. (2002) *Plant Cell* **14**, 3101-3117.

14. Pan, R., Lee, Y. R. & Liu, B. (2004) *Planta* **220**, 156-164.

15. Lee, Y. R., Giang, H. M. & Liu, B. (2001) *Plant Cell* **13**, 2427-2439.

16. Nishihama, R., Soyano, T., Ishikawa, M., Araki, S., Tanaka, H., Asada, T., Irie, K., Ito, M., Terada, M., Banno, H. *et al.* (2002) *Cell* **109**, 87-99.

17. Strompen, G., El Kasmi, F., Richter, S., Lukowitz, W., Assaad, F. F., Jurgens, G. & Mayer, U. (2002) *Curr. Biol.* **12**, 153-158.

18. Tanaka, H., Ishikawa, M., Kitamura, S., Takahashi, Y., Soyano, T., Machida, C. & Machida, Y. (2004) *Genes Cells* **9**, 1199-1211.

19. Hirokawa, N. & Takemura, R. (2004) *Exp. Cell Res.* **301**, 50-59.

20. Krendel, M. & Mooseker, M. S. (2005) *Physiology (Bethesda.)* **20**, 239-251.

21. Friml, J. & Palme, K. (2002) *Plant Mol. Biol.* **49**, 273-284.

22. Paponov, I. A., Teale, W. D., Trebar, M., Blilou, I. & Palme, K. (2005) *Trends Plant Sci.* **10**, 170-177.

23. Geldner, N., Friml, J., Stierhof, Y. D., Jurgens, G. & Palme, K. (2001) *Nature* **413**, 425-428.

24. Holweg, C. & Nick, P. (2004) *Proc. Natl. Acad. Sci. U S. A* **101**, 10488-10493.

25. Boutte, Y., Crosnier, M. T., Carraro, N., Traas, J. & Satiat-Jeunemaitre, B. (2006) *J Cell Sci.*

26. Steinmann, T., Geldner, N., Grebe, M., Mangold, S., Jackson, C. L., Paris, S., Galweiler, L., Palme, K. & Jurgens, G. (1999) *Science* **286**, 316-318.

27. Geldner, N., Anders, N., Wolters, H., Keicher, J., Kornberger, W., Muller, P., Delbarre, A., Ueda, T., Nakano, A. & Jurgens, G. (2003) *Cell* **112**, 219-230.

28. Friml, J., Yang, X., Michniewicz, M., Weijers, D., Quint, A., Tietz, O., Benjamins, R., Ouwerkerk, P. B., Ljung, K., Sandberg, G. *et al.* (2004) *Science* **306**, 862-865.

29. Benjamins, R. Functional analysis of the PINOID protein kinase in *Arabidopsis thaliana*. 2004. Leiden University.

30. Sambrook, J., Fritsch, F. & Maniatis, T. (1989) *Molecular Cloning - A Laboratory Manual* (Cold Spring Habour Laboratory Press, New York).

31. Guan, K. L. & Dixon, J. E. (1991) *Anal. Biochem* **192**, 262-267.

32. Chiu, W., Niwa, Y., Zeng, W., Hirano, T., Kobayashi, H. & Sheen, J. (1996) *Curr. Biol.* **6**, 325-330.

33. Gleave, A. P. (1992) *Plant Mol Biol* **20**, 1203-1207.

34. Neuteboom, L. W., Ng, J. M., Kuyper, M., Clijdesdale, O. R., Hooykaas, P. J. & van der Zaal, B. J. (1999) *Plant Mol. Biol.* **39**, 273-287.

35. Memelink, J., Swords, K., Staehelin, L. & Hoge, J. (1994) in *Plant Molecular Biology Manual*, eds. Gelvin, S., Schilperoort, R., & Verma, D. (Kluwer Academic Publishers, Dordrecht), pp. 1-26.

36. Schirawski, J., Planchais, S. & Haenni, A. L. (2000) *J Virol. Methods* **86**, 85-94.

37. Axelos, M., Curie, C., Mazzolini, L., Bardet, C. & Lescure, B. (1992) *Plant Physiol Biochem* **30**, 123-128.

38. Masson, J. & Paszkowski, J. (1992) *Plant J* **2**, 208-218.

39. Luschnig, C., Gaxiola, R. A., Grisafi, P. & Fink, G. R. (1998) *Genes Dev.* **12**, 2175-2187.

40. Clough, S. J. & Bent, A. F. (1998) *Plant J.* **16**, 735-743.

41. Reddy, A. S. & Day, I. S. (2001) *BMC. Genomics* **2**, 2.

42. Meyers, B. C., Lee, D. K., Vu, T. H., Tej, S. S., Edberg, S. B., Matvienko, M. & Tindell, L. D. (2004) *Plant Physiol* **135**, 801-813.

43. Zimmermann, P., Hirsch-Hoffmann, M., Hennig, L. & Gruissem, W. (2004) *Plant Physiol* **136**, 2621-2632.

44. Gingerich, D. J., Gagne, J. M., Salter, D. W., Hellmann, H., Estelle, M., Ma, L. & Vierstra, R. D. (2005) *J. Biol. Chem.* **280**, 18810-18821.

45. Du, L. & Poovaiah, B. W. (2004) *Plant Mol. Biol.* **54**, 549-569.

46. Bennett, S., Alvarez, J., Bossinger, G. & Smyth, D. (1995) *Plant J.* **8** , 505.

47. Benkova, E., Michniewicz, M., Sauer, M., Teichmann, T., Seifertova, D., Jurgens, G. & Friml, J. (2003) *Cell* **115**, 591-602.

48. Friml, J., Vieten, A., Sauer, M., Weijers, D., Schwarz, H., Hamann, T., Offringa, R. & Jurgens, G. (2003) *Nature* **426**, 147-153.

49. Li, J. & Chory, J. (1997) *Cell* **90**, 929-938.

50. Li, J., Nam, K. H., Vafeados, D. & Chory, J. (2001) *Plant Physiol* **127**, 14-22.

51. Sun, T., Goodman, H. M. & Ausubel, F. M. (1992) *Plant Cell* **4**, 119-128.

52. Weijers, D., Franke-van Dijk, M., Vencken, R. J., Quint, A., Hooykaas, P. & Offringa, R. (2001) *Development* **128**, 4289-4299.

53. Friml, J. (2003) *Curr. Opin. Plant Biol.* **6**, 7-12.

54. Blilou, I., Xu, J., Wildwater, M., Willemsen, V., Paponov, I., Friml, J., Heidstra, R., Aida, M., Palme, K. & Scheres, B. (2005) *Nature* **433**, 39-44.

55. Benjamins, R., Quint, A., Weijers, D., Hooykaas, P. & Offringa, R. (2001) *Development* **128**, 4057-4067.

56. Santner, A. A. & Watson, J. C. (2006) *Plant J* **45**, 752-764.